BTA/GE/14-04 **The behaviour of artificial archaeological remains during a one-dimensional compression test**

19-06-2014 **N.N. van Dijk**

Title	:	The behaviour of artificial archaeological remains during a one-dimensional compression test.
Author(s)	:	Nadine Nelleke van Dijk
Date	:	June 2014
Professor(s)	:	Dr.ir. D.J.M. Ngan-Tillard
Supervisor(s)	:	Dr.ir. D.J.M. Ngan-Tillard
TA Report number	:	BTA/GE/14-04

Postal Address	:	Section for Geo-Engineering Department of Geoscience & Engineering Delft University of Technology P.O. Box 5028 The Netherlands
Telephone	:	(31) 15 2781328 (secretary)
Telefax	:	(31) 15 2781189

The behaviour of artificial archaeological remains during a one-dimensional compression test

N. N. van Dijk

Delft University of Technology

Abstract

The Dutch subsoil contains a lot of archaeological remains that need to be preserved for future generations. Until now, it is not possible to predict if these remains will stay intact under the pressure of a manmade structure like an embankment. The goal of this research is to investigate the behaviour of assemblies of artificial archaeological remains during a one-dimensional compression test. The loads applied to the grains are similar to the loads under an embankment. Emmer wheat seeds, carbonized up to 270° C, 290° C and 370° C, have been assembled in a PEEK oedometer and were subjected to different loading stages with a maximum of 540 kPa. A total of four tests have been performed, one on each type of seed and a second test on the 290°C seeds, the latter being scanned with a micro CT-scanner in between every loading stage to be able to see individual grain behaviour in a 3D model. A comparison between the macroscopic yield stress (100 kPa for the second test on the 290° C grains) and the microscopic grain behaviour did not show clear resemblance because the point of yielding was not recognized in the 3D images.

Table of Contents

List of figures

List of tables

1 Introduction

This bachelor project aims at getting a better understanding of the influence of civil engineering structures on archaeological remains. The reason for this research lies behind the Treaty of Malta (1992), which states that our archaeological heritage must be better preserved. The basic principles of the Treaty of Malta are:

- In situ preservation of buried archaeological remains, the soil being the best guarantee for a good preservation.
- The possibility of presence of archaeological remains in spatial planning.

When building a civil engineering structure there are no tools available to predict whether or not damage will occur to the archaeological remains beneath. Therefore excavation and examination of the material are often requested. If it is possible to prove that an archaeological site will not be damaged when building a civil engineering structure on top of the site, excavation will not be necessary, time and money can be saved and the archaeological site can be preserved for future generations.

This project focuses on the behaviour of artificial archaeological remains, in the form of carbonized Emmer wheat seeds that are charred to different degrees of carbonization. The movement, rotation and breaking of the particles under pressure is studied. We performed one-dimensional compression tests (oedometer tests) on assemblies of seeds. The compression was applied in different stages and this loading simulates the conditions underneath the central part of an embankment built on top of a buried archaeological site. During one of the tests, a micro CT-scanner is used to create a three dimensional model of the assembly. By looking at the images of the micro CT-scanner, the behaviour of the grains at the different pressures is visible.

In the in situ conditions, the archaeological remains are surrounded by soft soils and the stress concentrations are lower due to more contact points. Therefore, the results of the tests we execute give a conservative estimate, in other words a worst case scenario.

1.1 Research questions

The main research question is:

- What is the behaviour of artificial archaeological remains under oedometric loading?

The rest of the questions can be divided into groups according to topic.

1.1.1 Stress-Strain

- What are the yield stresses of the different assemblies?
- Does the proposed procedure influence the macroscopic behaviour of the grains?

1.1.2 Visual observation

The research questions regarding visual observation can be subdivided in three categories; breaking, rotating, movement.

1.1.2.1 Breaking

- How do the particles break?
- At which stress or strain do the particles break?
- Do the particles break before, at or after the calculated yield stress?
- Which particles break first?
- Is fracture propagation through multiple grains in the sample visible?

1.1.2.2 Rotating

- Do the particles rotate?
- Does the rotation happen before or after breaking?
- Which particles rotate?

1.1.2.3 Movement

- Is rearrangement of the particles visible?
- Can we visually determine the loss of void ratio during the test?

1.2 Report structure

This report is divided into different chapters and in this section the structure of this document is explained.

Chapter 2 contains the literature review and is split in three parts: material, one-dimensional compression test, and visual observation. In the first part the knowledge about the artificial archaeological remains we used is presented, including how the material was obtained. The second part explains the one-dimensional compression test, specifically when performed on assemblies of particles, and the concept of yield stress. The third part is about visual observation of the material during or after testing.

Chapter 3 discusses the details of the different tests and equipments we used in this research. The working of the gas pycnometer, the one-dimensional compression test and the micro CT scanner are presented, including the used parameter settings.

Chapter 4 starts with the derivation of the macroscopic quantities that are needed to exploit the results of the tests. Furthermore, the chapter graphically shows the results of the latter tests and their interpretation.

Chapter 5 is about the image processing of the 3D scans. First the working of the program Avizo is explained and then three series of pictures are presented that were made with the program.

The report ends with a discussion of the results, conclusions and recommendations.

2 Literature study

The literature study focusses on three aspects: what is known about the material, what is known about one-dimensional compression tests on assemblies of particles, and which visual observation methods have been used by other researchers to study the influence of pressure on grain level.

2.1 Material

The material that is used consists of carbonized Emmer wheat seeds. The seeds are obtained from Mrs. G. Dolci from Monteleone di Spoleto, Italy. (van der Putte, 2011). From van Beurden (2002) we know that Emmer wheat has been cultivated in the Netherlands at least during the Neolithic (Pleistocene). One is therefore likely to encounter these seeds, in carbonized form, in the Dutch subsoil.

The process of artificial carbonization of the seeds we used in this research is extensively documented by van der Putte (2011). Van der Putte carbonized seeds at three different temperatures: 270^{o} C, 290^{o} C and 370^{o} C and assumed that the highest temperature would give the most charred, and therefore weakest, particles. We used all these three types of seeds in our research. The seeds are kept in sealed bags such that contact with air is prevented.

The charred wheat grains have an ellipsoid-shaped and are 3-5 mm long, 1-3 mm wide and thick. There is a groove over the entire length of the grain as can be seen in figure 1.

figure 1: Close-up picture of 290^{o} C grains after loading

2.2 One-dimensional compression test on assemblies of particles

One-dimensional compression tests on assemblies of particles have been performed before by e.g. Nakata et al. (2001) and Leleu & Valdes (2007). However, this test has not been executed on (artificial) archaeological remains. The results of the one-dimensional compression tests are usually presented in a void ratio e (volume of voids per unit volume of solids) against the logarithm of vertical effective stress σ_v' plot. Such a plot generally looks like the one in figure 2.

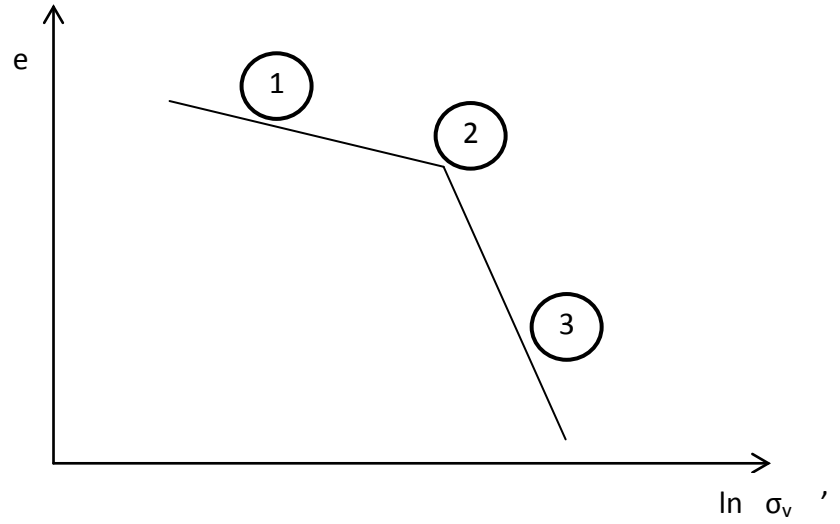

figure 2: Typical compression curve - void ratio (e) versus ln (σ_v')

In the plot above, the regions 1, 2 and 3 can be interpreted as "elastic stiffening", "yielding" and "plastic hardening" respectively (Bolton and McDowell, 1996). In region 1, particularly rearranging of particles is happening. The sample becomes stiffer because it densifies and deformations in this stage are partly recoverable. Region 2 marks the onset of particle breakage. The term (clastic) yielding is defined by Bolton and McDowell (1996) as: "*For a sample of uniform grains under compression, the sudden decrease in the rate of hardening, which is evident in region 2, must be due to the fracture of the weakest particles in the aggregate."* The yield point is estimated to be the point in the void ratio – log σ_v' graph with the highest curvature. Region 3 is reached after yielding and is named the normal compression phase. In this phase, the void ratio and the logarithm of the vertical stress show a linear correlation and the slope of this region is called compression ratio (CR). During this phase, particles break into smaller pieces which fill up empty space. This means that the void ratio reduces with increasing stress and the sample becomes stiffer.

The exact point of yielding depends on various factors, including single particle strength and the grading of the sample (Chuhan et al., 2003). The coordination number (number of contacts per particle) is also of influence on the point of yielding (McDowell and Bolton, 1998). When a particle has a high coordination number, the load on it is well distributed and the probability of fracture is much lower (Bolton and McDowell, 1996). This means more stress can be applied during a one-dimensional compression test before failure is reached and thus a higher yield stress. At lower (initial) void ratios, the average coordination number is higher, so the yield stress is higher.

Furthermore, McDowell and Bolton (1998) state that porous material shows a yielding region rather than a yield point. Since the carbonized wheat seeds are porous, we expect a more gradual curve in the void ratio – log σ_v' graph than the curve in figure 2.

2.3 Visual observation methods

It is desired to be able to look inside a sample while performing load tests. However, the combination of one-dimensional compression testing with micro CT scans has not been done before. Cheng et al (2001) studied thin (5mm) carbonate sand in a one-dimensional compression test through a glass plate. Through the glass, pictures were made and individual sand particles could be recognized. Although this

is a very good approach, this technique does not enable us to look at the grains in the middle of the sample but only at the ones that are pushed against the glass plate and are thus are influenced by a rigid boundary. Yamamuro et al. (1996) performed one-dimensional compression tests on sands at high pressures and made thin sections of the samples before and after the test. The thin sections were studied under a microscope. Although the thin sections do not show the exact same grains, one can assume that the behaviour of the individual grains during the test is the same for the whole sample. It would be more desired to see the same grains both before and after the test and in 3D. Therefore in our research we make use of the micro CT scanner.

3 Testing

In this research a total of three different tests are conducted. In this chapter the three tests, including the used equipment, are described and the used parameters are presented. The tests are:

- Gas pycnometer test – to define particle density
- One-dimensional compression test – to define macroscopic behaviour under pressure including yield stress
- Micro CT-scanner – to define the individual grain behaviour

3.1 The gas pycnometer

The apparatus we used in this research to determine the density is the Ultrapycnometer 1000 from Quantacrome. This pycnometer measures the true volume of a certain amount of granular or powdered material by employing Archimedes' principle of fluid (gas) displacement and the technique of gas expansion (Quantachrome, 2006). The used fluid is helium, which is chosen because of its small molecule size and its behaviour as ideal gas. From the weight of the sample and the volume, the density can be determined. For this research we measured both the density of the grains as well as the density of crushed grains, which were pulverized with a pounder. The grains are testes in a medium sized cell of 50 cm^3 with an accuracy of < ± 0.02% and the powders are tested in a small sized cell of 10 cm^3 with an accuracy of < ± 0.03%. The gas pycnometer performs ten runs for each volume measurement and the results of these runs are shown in table 1. A photograph of the pycnometer in operation is shown in figure 3.

table 1: The pycnometer results

Seeds	Grains/Powder	Cell Size	Weight (g)	Average volume (cm^3)	Average density (g/cm^3)
270° C	Grains	Medium	6.57	4.51	1.46
290° C	Grains	Medium	5.38	3.44	1.56
290° C	Powder	Small	2.71	1.82	1.49
290° C	Powder	Medium	14.11	9.59	1.47
370° C	Grains	Medium	4.94	2.92	1.69

If the intragranular voids would not be measured by the pycnometer, the tests performed on the grains would give a lower average density than the tests performed on the powder. However, since the opposite is true, we can conclude that the helium penetrates the grains and the pycnometer measures also the voids in the grains. Because of the powder being very fine material, and the possibility that part of it is carried away during the test or during the weighing, we consider the tests on granular material most reliable.

The variations in the results of the pycnometer test can be caused by the difference in the humidity of the air compared to the humidity of the grains. Since the grains are very dry, it is possible that they absorbed water from the air before or during the test. Another reason for the variations in the test results is that the carbonized material can have absorbed helium during the test. These difficulties lead to a less reliable test result.

figure 3: The gas pycnometer

3.2 The one-dimensional compression test

The one-dimensional compression test (oedometer test) is performed in a PEEK cylinder with inner diameter 60 mm and height 30 mm. PEEK is an organic thermoplastic polymer used in various engineering applications because of its excellent mechanical and thermal resistance properties. The PEEK cylinder is taped on a cylindrical surface with the same diameter as the outer diameter of the cylinder and together they form the oedometer. A solid, cylindrical top cap with diameter 59.7 mm is placed on top of the filled oedometer and acts as a loading cap, this top cap goes smoothly in the cylinder without causing side friction along the wall. The filled oedometer is placed in a very stiff load frame with a load cell of one kilo Newton and a displacement meter with 10 mm reach. The load cell of one kilo Newton is replaced by a load cell of five kilo Newton at the latest stage of the test. The test is displacement controlled and performed at a vertical compression rate of 0.1 mm per minute. The force produced in reaction to this compression rate is recorded. The one-dimensional compression test is performed at six different stages with unloading and reloading cycles. The top cap distributes the load equally over its surface and therefore we can calculate pressures from forces. A schematic representation of the test is shown in figure 4, and figure 5 presents a photograph of the load frame with the oedometer in operation. The different stages of the test can be found in table 2. The highest embankment in the western part of the Netherlands is probably the embankment built for the Prins

Claus crossing near Den Haag. This embankment has a height of 12 meters which represents a load of about 220 kPa.

We performed four one-dimensional compression tests. The 270^{o} C and the 370^{o} C grains were tested once and the 290^{o} C grains twice, of which the second test is interrupted after every unloading to make a scan. The latter test will be referred to as 290°-2 from now on. The details of the different tests are represented in table 3.

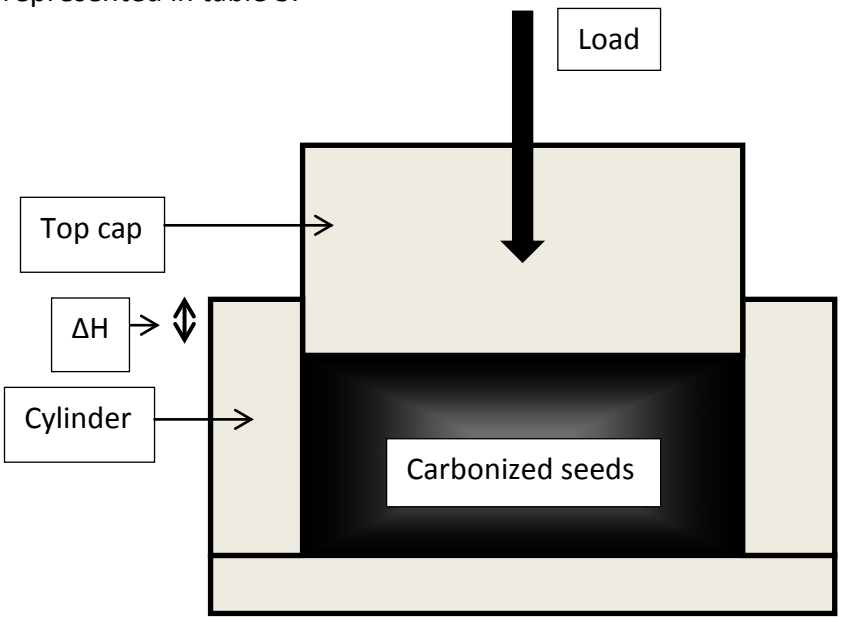

figure 4: Schematized test setup – The displacement ΔH is applied and the reaction force is measured

table 2: Compression stages

Force (N)	Corresponding pressure (kPa)
112	40
224	80
336	120
560	200
896	320
1456/1512	520/540

table 3: Test details

Date	Seeds	Details
26-4-2011	290° C	Up to 320 kPa
28-4-2011	270° C	Up to 540 kPa
2-5-2011 and 3-5-2011	290° C	With CT-scan in between every cycle, up to 520 kPa
17-5-2011 and 18-5-2011	370° C	Up to 320 kPa

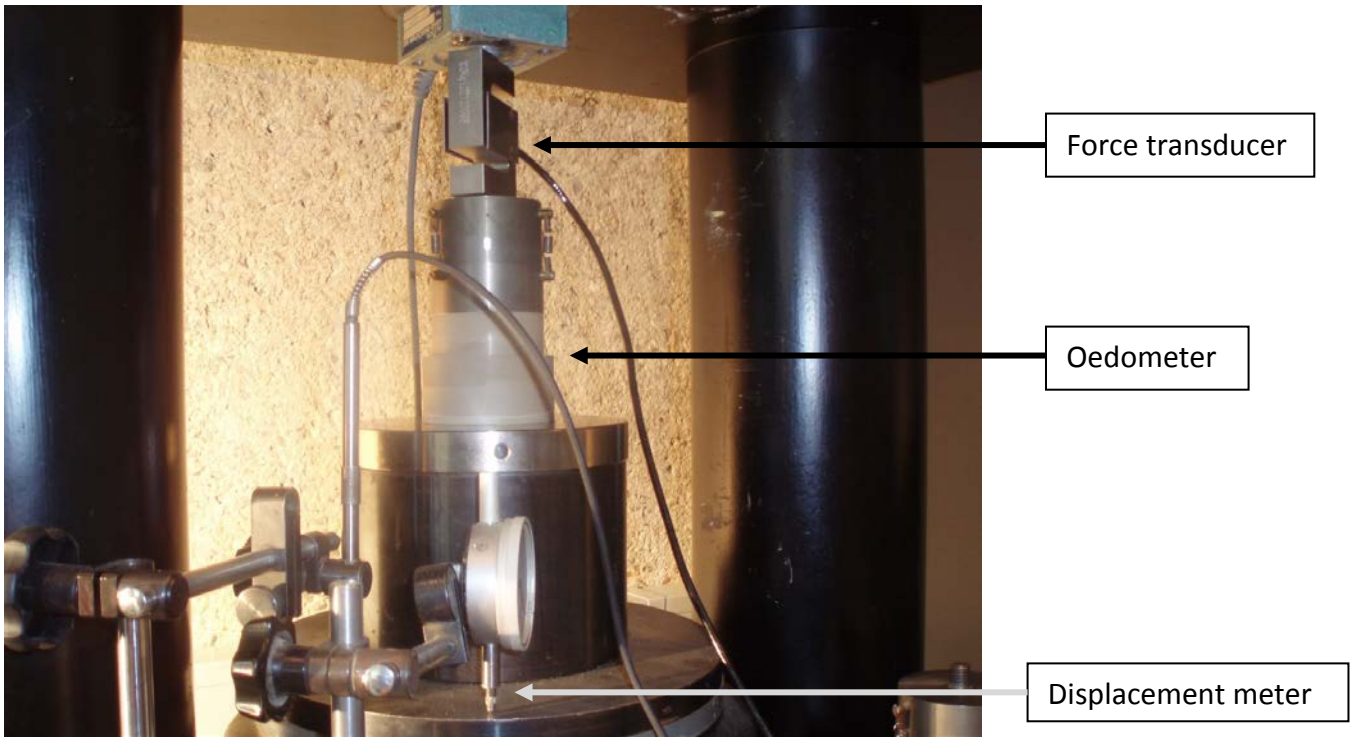

figure 5: The oedometer in the load frame

3.3 The micro CT-scanner

The micro CT-scanner used in this research is the Phoenix Nanotom s manufactured by GE (General Electric Company, 2013). The scanner is used to create 3D images of the sample. X-rays are emitted by the CT-scanner and go through the sample. After that, a camera records the X-rays that pass through the sample. A rotating device turns the sample with 0.25 degrees at a time which results in 1440 images. After aligning all these images a final 3D image is obtained with voxel size $2.16 \cdot 10^{-4}$ mm^3. We used this technique to be able to recreate a virtual sample without destroying the original sample. Before, after, and in between every unloading-reloading cycle of the one-dimensional compression test of the 290°-2 seeds, the whole sample, including the surrounding oedometer, is taken from the load frame and placed in the micro CT-scanner. In this way, the one-dimensional compression test could be continued after each scan. A picture of the micro CT-scanner is presented in figure 6.

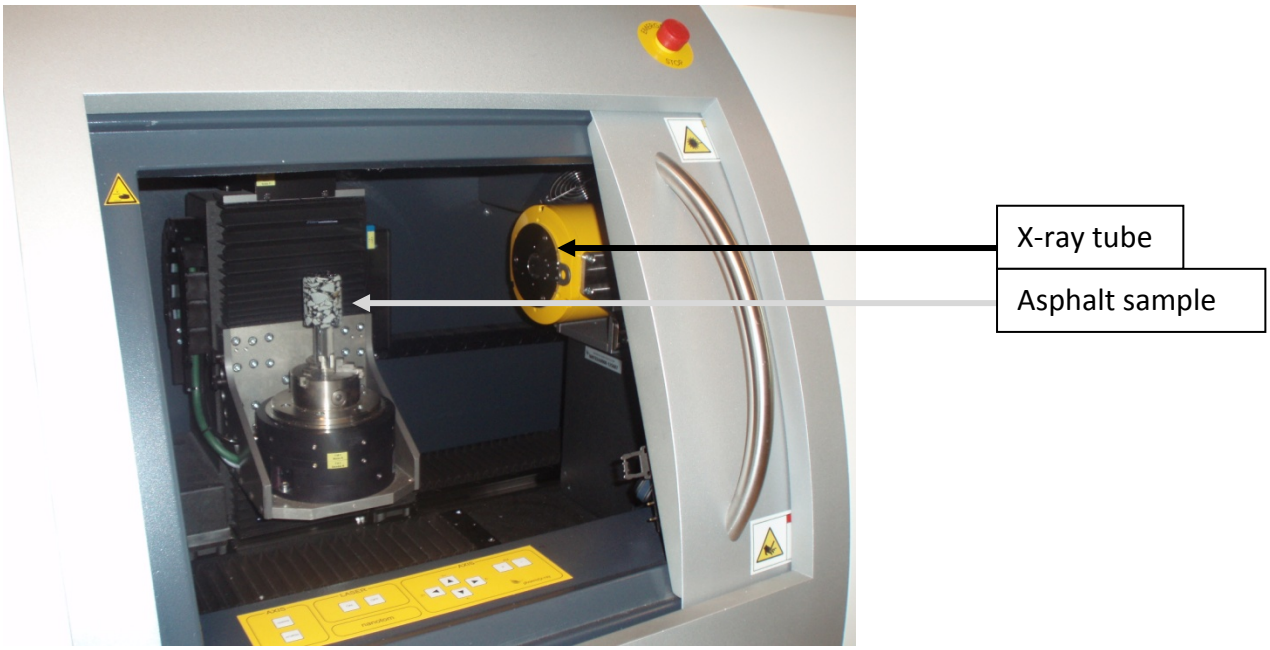

figure 6: The micro CT-scanner

4 Results of the one-dimensional compression tests

4.1 Derivation of quantities

From section 2.2 we know that results from one-dimensional compression tests are usually plotted in a void ratio – logarithm of mean effective stress diagram. This means that the outcomes of the test must be converted into these quantities. The pressure stages with their corresponding forces are given in table 2. Because the samples are totally dry, these pressures are equal to the vertical effective stresses. The derivation of the void ratio is not that simple. It needs to be split into two parts: derivation of initial void ratio and derivation of void ratio at any time but zero.

4.1.1 Derivation of initial void ratio

In the appendix the derivation of the formula for the initial void ratio is shown. The formula is also presented below.

$$e_0 = \frac{\rho_{grains}}{\rho_{packing\,(0)}} - 1$$

It can be seen that two different densities need to be known to be able to calculate the initial void ratio. The density of the packing can easily be calculated from the known volume of the oedometer (84.823 cm^3) and by measuring the mass of the whole sample. The density of the grains results from the pycnometer test. For the 290° C grains we take a grain density of 1.5632 g/cm^3. An overview of the used densities and the calculated initial void ratios of all samples is given in table 4.

table 4: Densities and initial void ratios of all samples

Sample	Mass (g)	Density sample (g/cm^3)	Density grains (g/cm^3) from pycnometer	Initial void ratio
270°	16.93	0.20	1.46	6.28
290°-1	16.86	0.20	1.56	6.86
290°-2	16.50	0.19	1.56	7.02
370°	12.91	0.15	1.69	10.14

4.1.2 Derivation of void ratio at time t

The void ratio at any time but zero depends on the vertical penetration. The vertical penetration is pressure dependent, and because the pressure changes with time, the vertical penetration also changes with time, and is referred to as $\Delta H_{(t)}$. This parameter is controlled and directly measured during the test. The derivation of the formula for the void ratio at time t is shown in the appendix. The resulting formula is:

$$e_{(t)} = e_0 - (e_0 + 1)\frac{\Delta H_{(t)}}{H_{(0)}}$$

We can only use this formula if we assume that displacement has only occurred in vertical direction. This means that we assume that the oedometer is completely stiff and that no horizontal deformation has occurred.

4.2 Observations and interpretation

As said before a total of four one-dimensional compression tests have been performed with the oedometer, on the 270° C grains, on the 370° C grains and two times on the 290° C grains. In this section the results of these tests will be shown. Each test is plotted on a different graph and an extra graph of both the 290° C tests is made to highlight the differences between these two tests. Also, an extra graph is made of the 270° C grains with the stress on a normal scale to show the stiffening of the sample.

4.2.1 270° C grains

The graphs in figure 7 show the results of the one-dimensional compression test performed on the 270° C grains. The vertical axis represents the void ratio, with the initial void ratio, calculated with zero stress, at the top of the graph. The void ratio reduces during the test because the sample gets pressed by the load frame. While the pressure (and thus the stress) increases, the volume of air in the sample reduces and therefore the void ratio reduces. The horizontal axis represents the induced stress, on a normal scale in figure 7a and on a logarithmic scale in figure 7b.

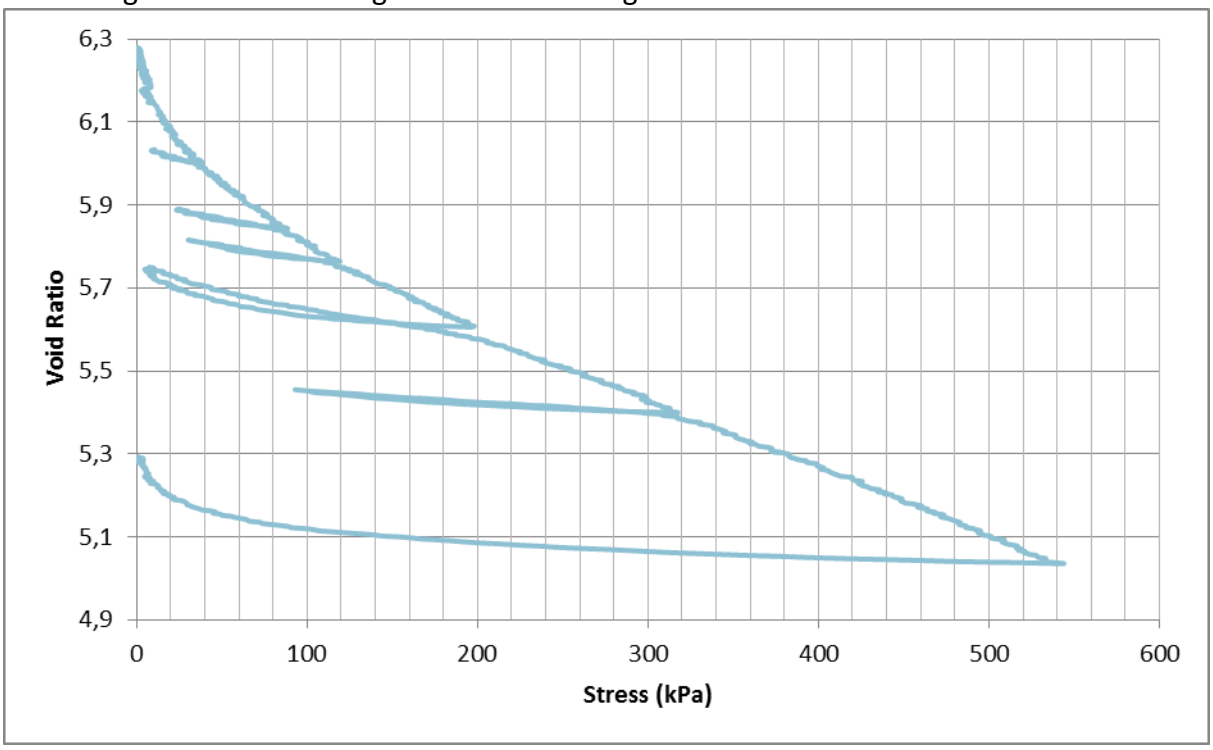

figure 7-a: One dimensional compression plot of 270° C grains, non-logarithmic

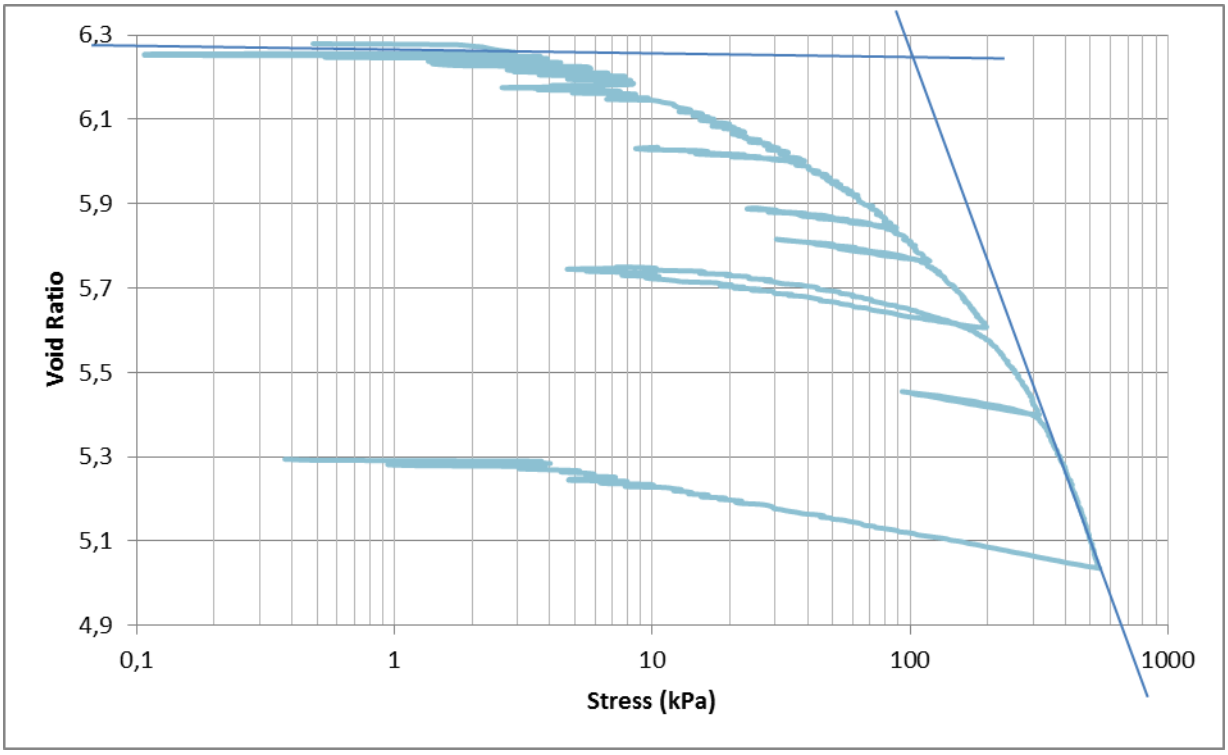

figure 7-b: One dimensional compression plot of 270° C grains

In figure 7a we see that the curve of the plot is the steepest at the beginning and gets less steep while the experiment continues. This means that the sample gets stiffer during the test, because it takes more force (i.e. a higher stress level) to reach the same decrease in void ratio. This phenomenon occurs in all tests and therefore we decided to show this graph (void ratio – stress) only once.

In figure 7b the three regions discussed in section 2.2 can be recognized, however the point of yielding is not so easy to distinguish because the graph is more curved than the one in figure 2. To determine the point of yielding, it is commonly accepted by geotechnical engineers to take the intersection of the tangents of the first and third region. This is found to be at 100 kPa. The graph in figure 7b also shows the unloading-reloading cycles as described in 3.2. It can be seen that during unloading of the sample, part of the void ratio is recovered (elastic strain) but most part is unrecoverable (plastic strain).

4.2.2 290° C grains

The results of the first test with the 290° C grains are presented in the graph in figure 8. This graph looks similar to the one in figure 7b but the initial void ratio is higher. The yield stress is 80 kPa, which is lower than the yield stress of the 270° C grains. The difference in yield stress can have two causes. On one hand, the 290° C grains are more carbonized than the 270° C grains and therefore it can be assumed that the former grains are weaker. Besides that, from the literature study we know that yield stress reduces with increasing initial void ratio.

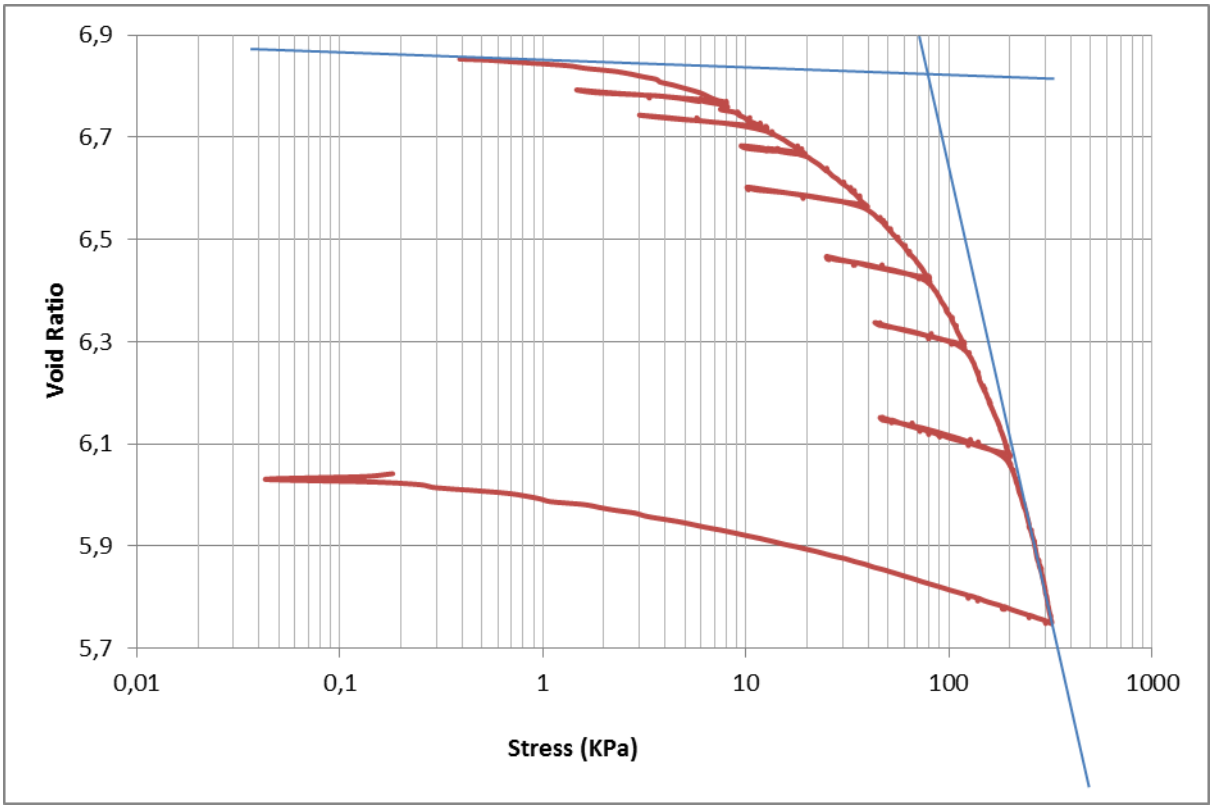

figure 8: One dimensional compression plot of 290° C grains, test 1

The graph of the second test of the 290° C grains, presented in figure 9, shows a different behaviour than the graph of the first test in figure 8. First of all, to be able to make a scan of the sample, full unloading was necessary, while during the previous tests, the samples were only partly unloaded. The 'gaps' in the curve of figure 9 show that particles rearrangement has occurred while the sample was unloaded. It is possible that transportation of the sample from the load frame to the micro CT scanner caused shaking of the sample and this may have resulted in rearrangement of grains.

Another explanation for the gaps in the graph is the long exposure to air. It took a few hours to make a scan and therefore the whole test took two days. This in contrary to the first test of the 290° C grains, which took only a couple of hours. The charred particles could have absorbed water from the air in the meantime.

bla
Each time reloading started, the displacement meter needed to be set at zero. Afterwards, the measured vertical penetration from before the scanning was added up to the penetration after the scanning. This operation was necessary to connect the data and to make a continuous graph. By doing this operation, we assume no change in vertical displacement, and thus no change in void ratio, during the scanning.

The yield stress of the second test of the 290° C grains is estimated to be 100 kPa.

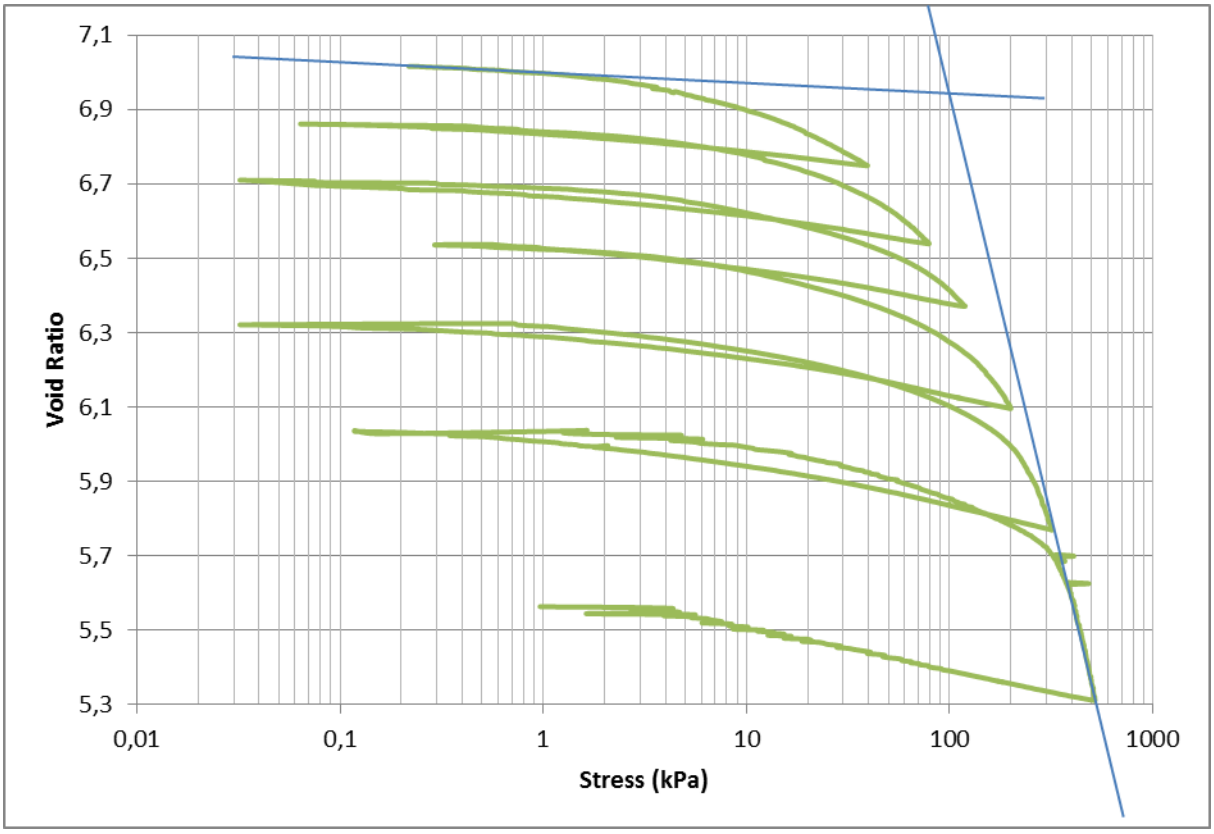

figure 9: One dimensional compression plot of 290° C grains, test 2

In figure 10 the graphs of figure 8 and figure 9 are plot on the same scale. We can now clearly see the differences between the two graphs. The initial void ratio of the second test (green graph) is higher than the initial void ratio of the first test (red graph). Although McDowell and Bolton (1998) state that a higher initial void ratio will lead to a lower yield stress, this is not what we see in the results in figure 10 because the yield stress of the second test is in fact higher than the yield stress of the first test. This means that the test procedure of the second test, i.e. the scanning, is of influence on the yield stress.

The first test with the 290° C grains (red curve in figure 9), is only performed to a maximum pressure of 320 kPa. This makes it difficult to predict whether the At high stresses, both curves converge to each other.

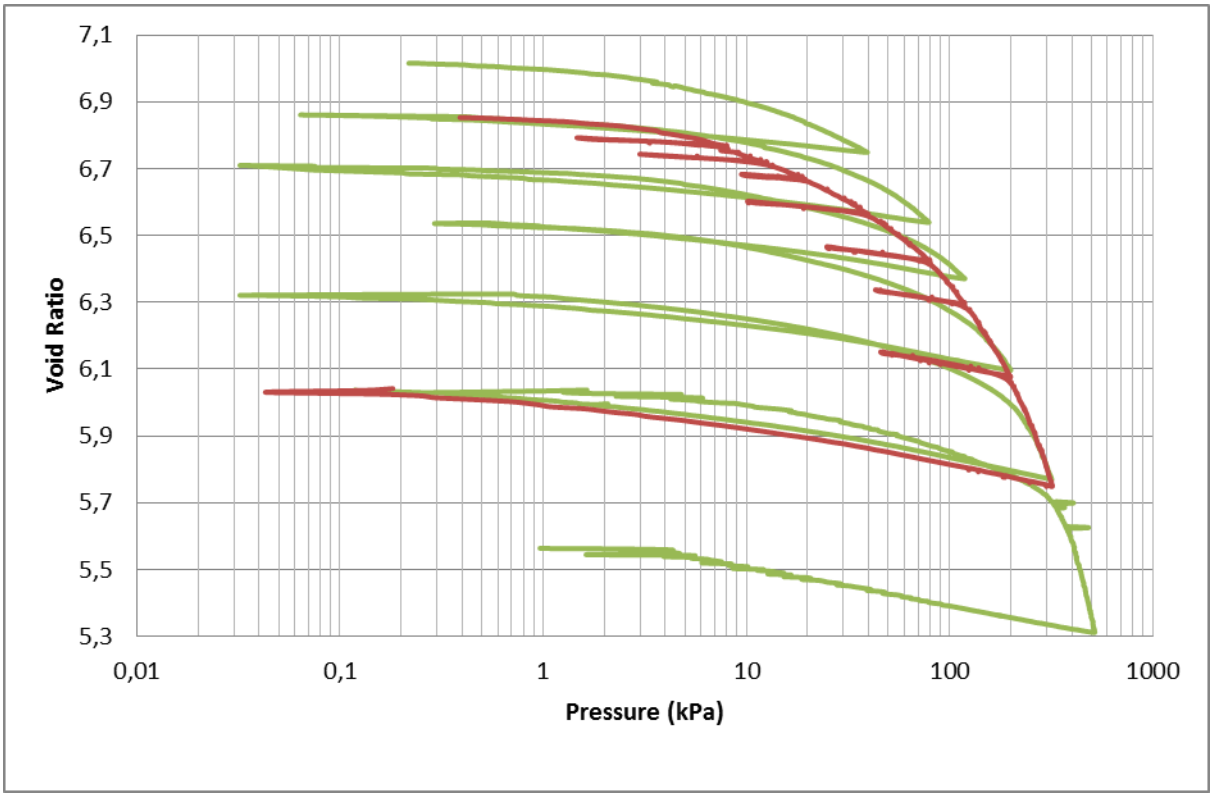

figure 10: One dimensional compression plots of both 290° C grains tests (test 1 in red, test 2 in green)

4.2.3 370° C grains

The graph representing the results of the 370° C grains test is shown in figure 11. The yield stress of this sample is estimated to be 25 kPa which is substantially lower than the yield stresses of the previous tests. During the test of the 370° C grains, the void ratio is almost halved and the third compression stage is reached a lot earlier than during the other tests. Likewise, the test with the 370° C grains took a lot longer because the test was still displacement controlled with a rate of 0.1 mm per minute. Hence, the execution of the test took two days with a break between the stage of 120 kPa and 200 kPa. This overnight break shows its influence with a gap in the curve and this supports our idea that long exposure to air has influence on the results of the test.

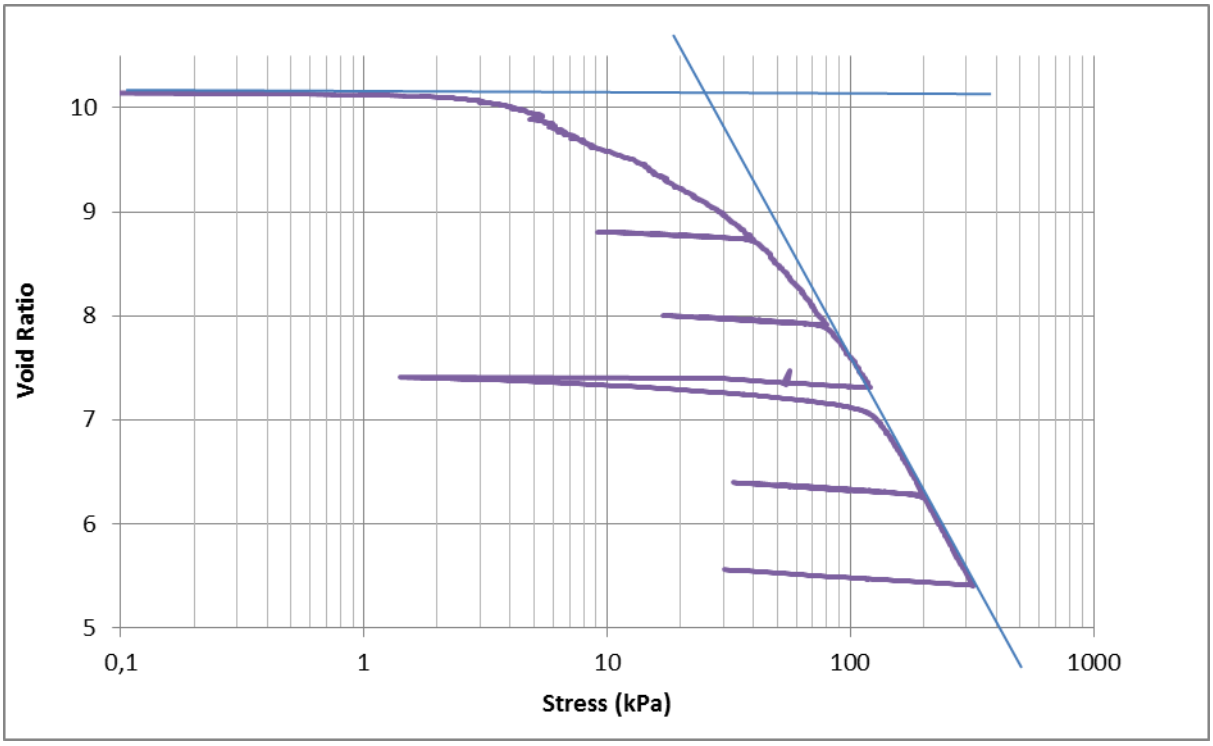

figure 11: One dimensional compression plot of 370° C grains

5 Image processing

5.1 Introduction

The sample of test 290-2 was put in a micro-CT scanner before the one-dimensional compression test, after the test and in between every unloading-reloading cycle. In this way, a total of seven scans are made. We processed the results of these scans with the program Avizo, which is a software application for data visualization and analysis. Three areas near the central axis of the sample were looked at in detail, namely at the top, bottom and the middle of the sample. In this chapter, the results of the scans will be discussed.

5.2 Avizo

The program Avizo has a lot of tools to process and analyse 3D pictures, such as filtering, smoothing, grain separation and surface generation. However, due to little contrast of the particles on the images, as well as the presence of dust and very fine material in the sample, it was not so easy to use these tools well. Wrong particle segmentation occurred, i.e. particles stuck together or were cut in half while trying to perform particle separation. Due to the complex external and inner shape of the particles, we were not able to visualize particle surfaces in the case where one particle penetrated another (broken) particle. Another problem that occurred was that the intragranular voids were not recognised as such when we tried to calculate the volume of grains per slice so we were not able to verify the calculated void ratio by optical means. That is why we decided to look only at the raw images.

5.3 Image observation and interpretation

Three areas near the central axis of the sample are investigated and the observations are discussed. A series of seven pictures, one per loading stage, of every area is presented of which the final picture (after the highest stress) is enlarged to show clearly the development of grain damage during the test.

5.3.1 Grains at the top of the sample

The picture series of the central area at the top of the sample is shown in figure 12. The series focusses on one grain and shows the movement of that grain, including contacts with neighbour grains, during the test. The diameter of the grain is roughly 3.7 mm, as indicated on the pictures. The pictures show a vertical cross section and are taken at a fixed level. The black part at the top of the pictures is the top cap of the oedometer. It is clearly visible that the top cap is moving downwards during the test, meaning vertical penetration. The centered particle is also moving downward, this can be seen by the contours of the start position of this grain.

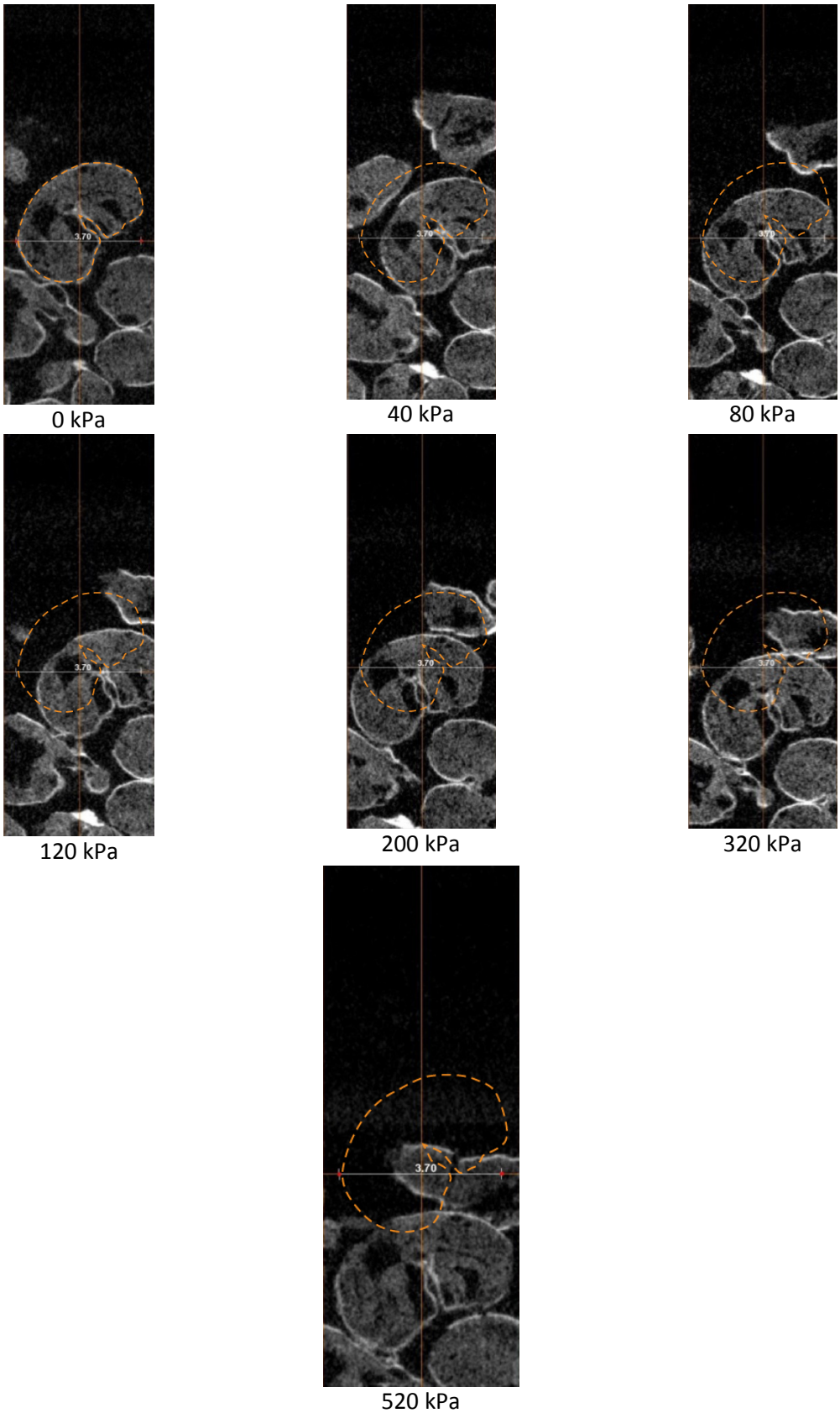

figure 12: Picture series of 290° C grains at the top of the sample

Although one would expect that the top cap of the oedometer, which is a rigid boundary, would give the grain less degrees of freedom, yet it is possible for the grain to rotate 25°. It can be seen that the grains are being pushed against each other and that the intergranular space is reduced during the test. This

leads to an increase in coordination number, and hence, to a more equally distribution of the increased stress. The centered grain does not break during the test nor shows signs of cracks.

Because the diameter of the grains is large with respect to the sample diameter (3.7 mm versus 60 mm), it is difficult to make a homogeneous top surface. As a result, the initial packing at the top of the sample is higher than in the rest of the sample.

5.3.2 Grains at the bottom of the sample

The pictures of figure 13 show a grain at the bottom of the sample. The light grey part at the bottom of the pictures is the bottom of the oedometer. As in figure 12, the orientation of the pictures is vertically.

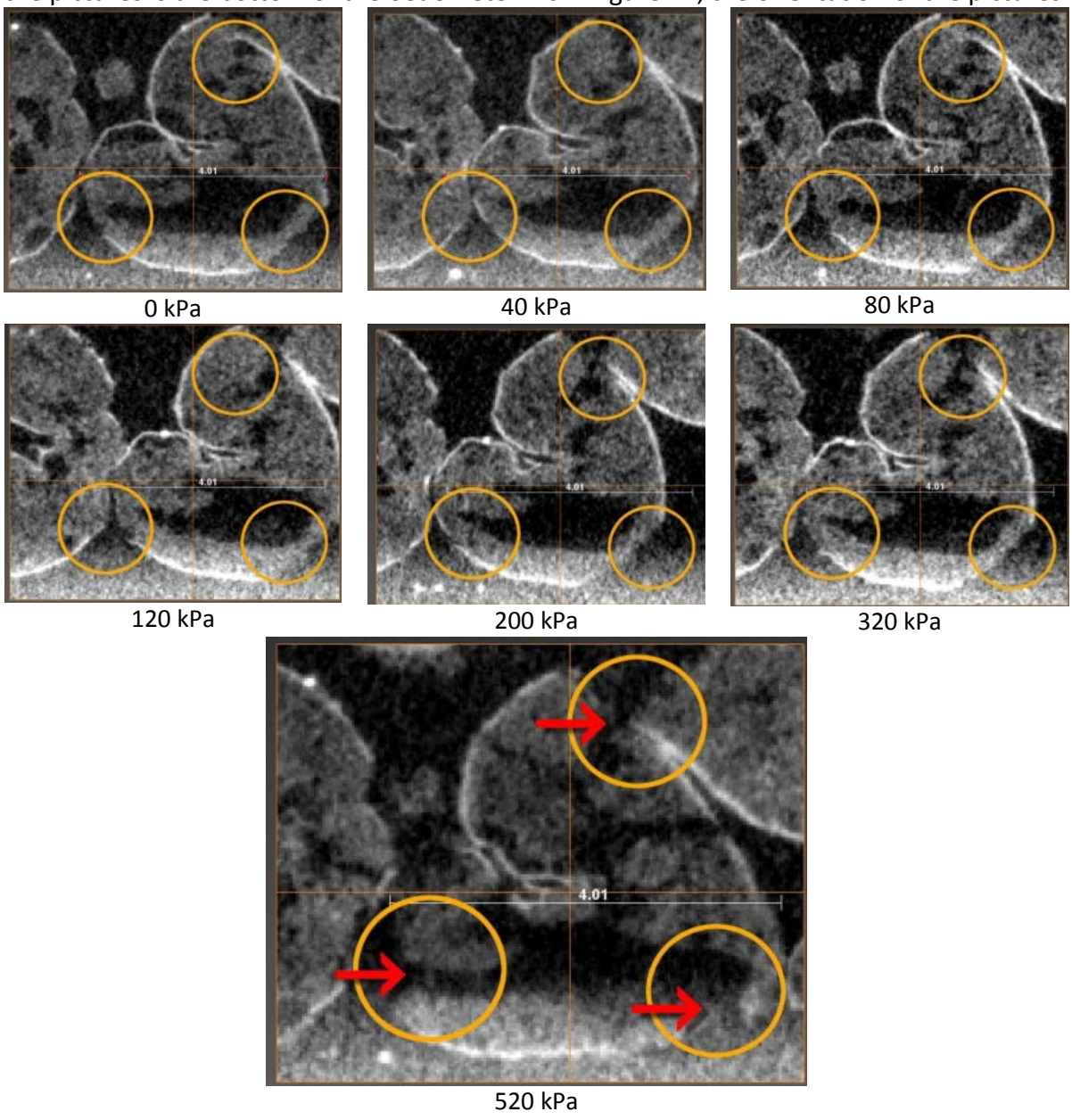

figure 13: Picture series of grains° C at the bottom of the sample

The grain at the bottom of the sample has few degrees of freedom due to the rigid boundary and this keeps the grain from rotating. Unlike the area at the top of the sample, at the bottom there seems to be little decrease of intragranular voids and no change in coordination number. It might be that the sample was already more dense at the bottom at the beginning of the test due to manual sample preparation.

The circles in the pictures of figure 13 show the points of interest, which are the contact points of the centered grain with either other grains, or the rigid boundary. At these points the grain starts to break. The first crack can be seen at 320 kPa and at 520 kPa there are cracks at all contact points and these cracks lead to a decrease in intragranular porosity.

5.3.3 Grains at the middle of the sample

The picture series of an area at the middle of the sample is shown in figure 14. Unlike the pictures in figure 12 and figure 13, figure 14 shows horizontal cross sections. The pictures are not taken at the same level but are set to show more or less the same cross sections of the grains in every picture. The scale of the pictures is best shown at the 520 kPa picture, where the cross section of one of the grains is roughly 3 mm.

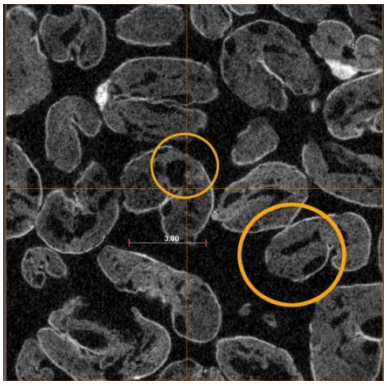

0 kPa

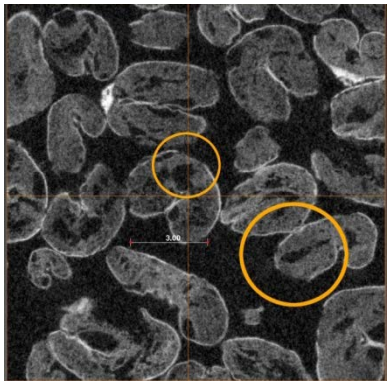

40 kPa

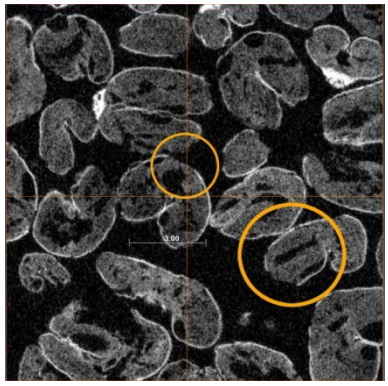

80 kPa

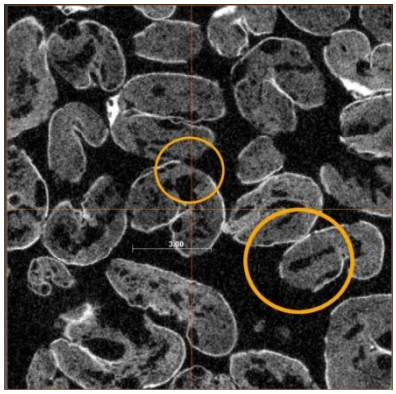

120 kPa

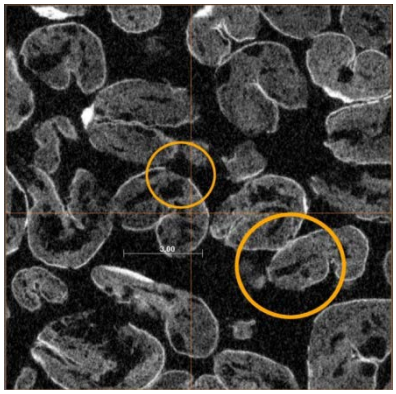

200 kPa

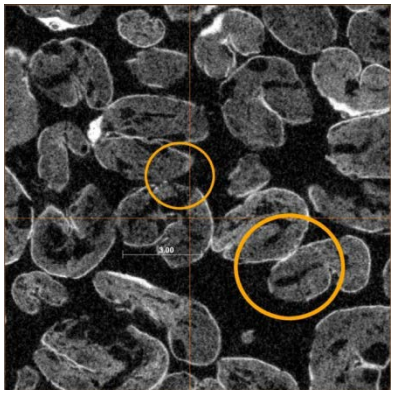

320 kPa

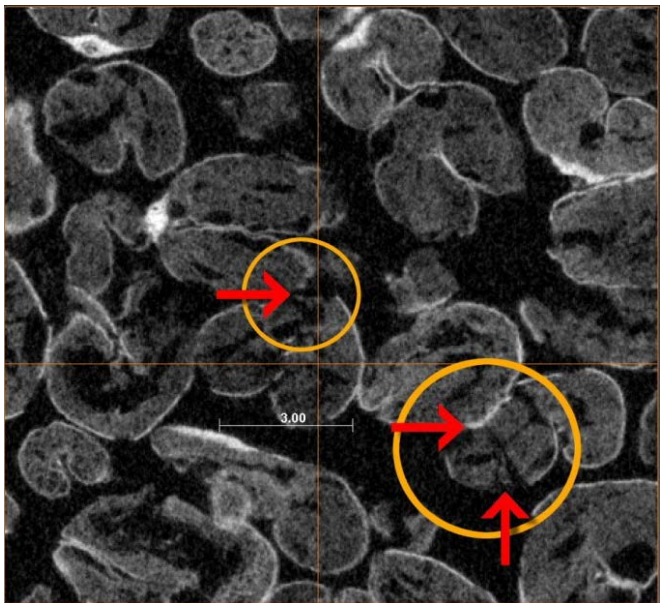

520 kPa

figure 14: Picture series of grains^{o} C at the middle of the sample

In the middle of the sample there is little or no influence of any boundary and there does not seem to be much rotation of particles. The intergranular porosity is still high at 520 kPa. Also, at 520 kPa a lot of grains are still intact and only two grains show clear damage as indicated by the orange circles. The grain in the top circle shows the first damage at 320 kPa when the grain next to it is being pushed against it. The first crack initiates at the contact point. The same happens in the lower orange circle, but here the first crack is visible only at 520 kPa. The grains in both circles show closure of cavities and thus a reduction of intragranular porosity with an increase in fractures.

Because only two of the visible grains show damage, nothing can be said about propagation of fractures through the multiple grains in the sample and neither can it be said whether bigger or smaller grains break first.

6 Discussion

The yield stresses of the four different samples are summarized in table 5. From the literature study in 2.2 we know that the yield stress marks the beginning of breaking of individual particles, so one can say that the macroscopically determined yield stresses of table 5 are the maximum allowed pressures on archaeological sites. However, these yield stresses proved to be unreliable when looking at the damage of the particles because fracturing of grains is only visible at the scans of 320 kPa and 520 kPa. This disparity can be caused by imprecision in the manual determination of the yield point or by the local behaviour in the sample. It is possible that grains in other parts of the sample break at an earlier stage, but such grains were not seen on the scans.

table 5: Calculated yield stresses of all samples

Sample	**Yield stress (kPa)**	**Load step at which first grain damage is detected (kPa)**		
		Top of the sample	**Middle of the sample**	**Bottom of the sample**
270^{o} C	100			
290^{o} C, test 1	80			
290^{o} C, test 2	100	-	320	320
370^{o} C	25			

The images of the micro CT scanner clearly show grain behaviour on microscopic level. The figures in 5.3 show rotation, fracturing and movement of the individual grains and also the exact starting points of the fractures can be tracked. From this, we can conclude that using micro CT images is profitable in the determination of individual grain behaviour during one-dimensional compression tests. On the other hand, the procedure we used (loading, unloading, taking sample to micro CT scanner, scanning, taking sample back to load frame, reloading, etc.) influences obviously the results of the one-dimensional compression test as indicated in figure 10 and leads to a difference in yield stress of 20 kPa between the test with scans and the one without scans. It would be beneficial if it is possible to change the circumstances of the scanning procedure such that the interruption of the one-dimensional compression test does not have as much impact on the results as before.

7 Conclusions and recommendations

Because the used procedure influences the result of the one-dimensional compression test we recommend improving the test procedure. It would be better if translocation between the load frame and the micro CT scanner could be minimized. Also, long term exposure to air must be prevented as much as possible and this may be possible by adjusting the compression speed or the scanning time.
Another recommendation is to perform test with grains embedded in different soft soils to have a better understanding of in situ conditions.

References

Beurden, L. van, 2002: Botanisch onderzoek in het Maas-Demer-Scheldegebied. De Romeinse en vroegmiddeleeuwse periode. *In: Fokkens, H. en Jansen, R. (red.), in: 2000 jaar bewoningsdynamiek. Brons- en ijzertijdbewoningin het Maas-Demer-Schelde gebied, Leiden, 287-314*

Bolton, M.D. & McDowell, G.R. (1996). Clastic mechanics. *IUTAM symposium on mechanics of granular and porous materials* (ed. N. A. Fleck and A. C. F. Cocks). Dordrecht: Kluwer.

Cheng, Y.P., White, D.J., Bowman, E.T., Bolton, M.D. & Soga, K. (2001). The observation of soil microstructure under load. *4th international conference of micromechanics of granular media, powders and grains* 2001, Sendai, Japan

Chuhan, F.A., Kjeldstad, A., Bjorlykke, K., & Hoeg, K. (2003). Experimental compression of loose sands: relevance to porosity reduction during burial in sedimentary basins, *Can. Geotech.* J. 40: 995-1011
Leleu, S.L. & Valdes, J.R. (2007). Experimental study of the influence of mineral composition on sand crushing. *Géotechnique* 57, No. 3, 313-317

General Electric Company (2013). *Phoenix nanotom m* [Brochure]. Retrieved from www.ge-mcs.com.

McDowell, G.R. & Bolton, M. D. (1998). On the micromechanics of crushable aggregates. *Géotechnique* 48, No. 5, 667-679

Nakata, Y., Hyodo, M., Hyde, A.F.L., Kato, Y., Murata, H. (2001). Microscopic particle crushing of sand subjected to high pressure one-dimensional compression. *Soils and Foundations*, Vol. 41, No. 1, 69-82

Putte, E. van der, (2011). The strength of carbonized wheat. BSc thesis, TuDelft

Quantacrome Instruments (2006). *Quantachrome Pycnometers Automatic* [Brochure]. Retrieved from http://www.quantachrome.com.

Yamamuro, J.A., Bopp, P.A., Lade, P.V. (1996). One-dimensional compression of sands at high pressures. *Journal of geotechnical engineering*, Vol. 122, No. 2

Appendix

Derivation of a formula for the void ratio

The void ratio is defined by the volume of the pores divided by the volume of the grains.

$$\text{e (void ratio)} = \frac{V_{pore}}{V_{grains}} = \frac{V_{sample} - V_{grains}}{V_{grains}}$$

Volume can be written as mass over density and thus follows:

$$= \frac{\frac{m}{\rho_{packing}} - \frac{m}{\rho_{grains}}}{\frac{m}{\rho_{grains}}}$$

The density of the packing is time dependent; it depends on ΔH, the vertical penetration. Multiplying this equation by the density of the grains gives:

$$= \frac{\frac{m \cdot \rho_{grains}}{\rho_{packing\,(t)}} - m}{m}$$

Dividing this equation by m:

$$= \frac{\rho_{grains}}{\rho_{packing\,(t)}} - 1 \qquad (1)$$

The initial void ratio can be found by taking the equation above at time zero.

$$e_0 = \frac{\rho_{grains}}{\rho_{packing\,(0)}} - 1 \qquad (2)$$

The density of the packing is unknown at all times except at time zero. Therefore we need to find an expression for the density of the packing.

$$\rho_{packing\,(t)} = \frac{m}{V_{sample\,(t)}} = \frac{m}{H_{(t)} \cdot A}$$

In which A represents the surface area of the oedometer. The height of the sample can be calculated by subtracting the vertical penetration from the initial height, and so the equation becomes:

$$= \frac{m}{(H_{(0)} - \Delta H_{(t)}) \cdot A} = \frac{m}{H_{(0)} \cdot A - \Delta H_{(t)} \cdot A} = \frac{m}{A} \cdot \frac{1}{H_{(0)} - \Delta H_{(t)}}$$

By factoring out the initial height we get:

$$= \frac{m}{A} \cdot \frac{1}{H_{(0)}\left(1 - \frac{\Delta H_{(t)}}{H_{(0)}}\right)} \qquad (3)$$

At time zero, the vertical penetration is also zero. Thus the initial packing can be written as:

$$\rho_{packing(0)} = \frac{m}{A \cdot H_{(0)}} \qquad (4)$$

Combining (3) and (4) gives:

$$\rho_{packing(t)} = \rho_{packing(0)} \cdot \frac{1}{1 - \frac{\Delta H_{(t)}}{H_{(0)}}} \qquad (5)$$

We can now enter equation (5) into equation (1) to get an expression for the void ratio.

$$e_{(t)} = \frac{\rho_{grains}}{\rho_{packing(0)} \cdot \frac{1}{1 - \frac{\Delta H_{(t)}}{H_{(0)}}}} - 1 = \left[\frac{\rho_{grains}}{\rho_{packing(0)}} \left(1 - \frac{\Delta H_{(t)}}{H_{(0)}} \right) \right] - 1$$

By expanding the previous equation we get:

$$= \frac{\rho_{grains}}{\rho_{packing(0)}} - \frac{\rho_{grains}}{\rho_{packing(0)}} \cdot \frac{\Delta H_{(t)}}{\Delta H_{(0)}} - 1 \qquad (6)$$

A part of (6) is equal to the formula for the initial void ratio (1), these two combined gives:

$$= e_0 - \frac{\rho_{grains}}{\rho_{packing(0)}} \cdot \frac{\Delta H_{(t)}}{H_{(0)}} \qquad (7)$$

Equation (1) can be rewritten as:

$$e_0 + 1 = \frac{\rho_{grains}}{\rho_{packing(0)}} \qquad (8)$$

And so we can substitute a part of (7) by (8) and this leads to the final formula for the void ratio.

$$e_{(t)} = e_0 - (e_0 + 1) \frac{\Delta H_{(t)}}{H_{(0)}} \qquad (9)$$